Radio Science, Volume ???, Number , Pages 1–16,

Space-Time Ambiguity Function in 3-D ISR

John Swoboda,[1] Joshual Semeter,[1] Philip Erickson[2]

Corresponding author: J. P. Swoboda, Department of Electrical & Computer Engineering, Boston University, 8 Saint Marys Street Boston, MA 02215, USA. (swoboj@bu.edu)

[1]Department of Electrical & Computer Engineering, Boston University, Boston, Massachusetts, USA.

[2]Atmospheric Science Division, MIT Haystack Observatory, Westford Massachusetts, USA.

By leveraging electronically steerable phased array antenna technology, incoherent scatter radars have now become full three-dimensional remote sensors for ionosphere plasmas. Currently these systems are operating in the high latitude region where the ionosphere is highly dynamic in both space and time. These systems are giving researchers an unprecedented look at the ionosphere that they have not had in the past.

Because of the highly dynamic nature of the ionosphere in this region it is import to differentiate between artifacts and the true behavior of the plasma. Often the three dimension data is fitted in polar coordinates and then the parameters are interpolated to a Cartesian grid. This and other sources of error could be effecting reconstructions of the plasma parameters

In this study we explore the impacts of fast moving plasma progressing through the field of view of the radar on the reconstruction of the three dimensional parameters. We pose the problem as a linear inverse problem for the lags of the plasma autocorrelation function. We will show the impact of the plasma through simulation from a full 3-d incoherent scatter radar model. From there we can apply methods from image and video processing to attempt to correct for the artifacts.

1. Introduction

Incoherent scatter radar (ISR) systems have enabled researchers since the 1950's to explore the ionosphere *Gordon* [1958]. Using methodology developed by Dougherty, Farley and others these systems can give measurements of electron density N_e, Ion temperature T_i, electron temperature T_e, Ion velocity V_i and other plasma parameters *Dougherty and Farley* [1960], *Farley et al.* [1961], *Hagfors* [1961], *Dougherty and Farley* [1963]. These parameters are measured by fitting a theoretic autocorrelation derived from first principles physics to an estimated intrapulse time autocorrelation of the scattered radar signal *Lehtinen and Huuskonen* [1996].

As with any real world measurement method there is a non-ideal measurement ambiguity which gives these sensors a type of resolution. Often these ambiguities are only carried out over range and time. The range ambiguity is controlled by the pulse shape and the time ambiguity is controlled by the integration time. A number techniques have been developed to reduce the impact of these ambiguities including full profile analysis *Holt et al.* [1992]. *Lehtinen* [1989], *Lehtinen et al.* [1997] and deconvolution methods *Nikoukar et al.* [2008].

Recently phase array technology has started to be leveraged by ISR community. The AMISR systems have already been deployed both at the Poker Flat Alaska and Resolute Bay Canada ami [2014]. The EISCAT-3D project is currently being developed using phased array technology as well and will be capable of multistaic processing eis [2005]. These new systems are already being used to create three

dimensional reconstructions of plasma parameters *Semeter et al.* [2009], *Nicolls and Heinselman* [2007], *Dahlgren et al.* [2012a],*Dahlgren et al.* [2012b].

Even though these systems are already in use there is no formal derivation of a three dimensional ambiguity function for these systems. In a highly dynamic region like the high latitude ionosphere this lack of knowledge can be problematic. There are numerous phenomena such as polar cap patches that may be moving through the field of view at very high speeds *Dahlgren et al.* [2012a].

These three-dimensional reconstructions often consist of taking the fitted parameters and then interpolating them to a Cartesian space from the system's natural spherical coordinate space *Butler* [2013]. The step of fitting the autocorrelation function to the theoretical functions to find the final plasma parameters is a non-linear operation. Because of this it is impossible to exactly predict the impact on the parameter values as different plasma populations move through the field of view of the radar. Alternatively it is possible to treat the formation of the autocorrelation estimates as a linear process with each lag as an independent channel *Nikoukar et al.* [2008].

In this publication we will develop a model for a full three dimensional space-time ambiguity function for 3-D ISR systems. This function can also be modified to show the ambiguity within the rest frame of the moving plasma. In the end this full three dimensional can be represented as kernel in a Fredholm integral equation like in Equation 1 with $f(s)$ being the lag of the autocorrelation function at a specific time and position.

$$g(t) = \int_a^b K(t,s)f(s)ds \tag{1}$$

The impact of the three-dimensional ambiguity on moving plasma will be shown through simulation. This ISR simulator fully emulates the ISR data creation process at the IQ level.

Lastly possible mitigation techniques will be explored. These mitigation techniques will borrow heavily from the image and signal processing literature.

2. Space-Time Ambiguity

In the ISR literature the measurement ambiguity along the range dimension is often referred to simply as the ambiguity function *Hysell et al.* [2008]. This only shows the measurement ambiguity along the range r. Due to the three-dimensional imaging capability of phased array ISR systems we will define a new set of terminology to describe this more complicated measurement which is now imaging the ionosphere in three-dimensional coordinates $\mathbf{r} = [x, y, z]^T$. We will represent the sampled coordinates within the radar with $_s$ such as $\mathbf{r}_s$.

Specifically we will refer to the measurement ambiguity in the range dimension as the range ambiguity, $W(r, r_s, \tau)$. The measurement ambiguity in the elevation and azimuth angles will be referred to as the angular or cross range ambiguity $F(\theta, \phi, \theta_s, \phi_s)$, where θ is the physical elevation angle, ϕ is the physical azimuth angle, θ_s is the elevation angle that the radar is pointing at and ϕ_s is the azimuth angle that the radar is pointing at. The since these two functions are separable they can be multiplied

together to form the full spatial ambiguity $K(\tau, \mathbf{r}, \mathbf{r}_s)$. Lastly integration time for each measurement will be referred to the time ambiguity. Again like the full spatial ambiguity function we can multiply the space and time ambiguity functions to get the Space-Time ambiguity function which will be represented as $A(\tau, \mathbf{r}_s, \mathbf{r}, t_s, t)$.

2.1. Derivation

In order to develop the space-time ambiguity we will use two different sets of time commonly known in radar literature as fast-time n and slow-time t. Fast-time looks at time on the order of the radar systems A/D conversion while slow-time time is looking at time on the order of the system's pulse repetition interval *Richards* [2005]. We will use the same reference for fast-time but slow time will be the time it takes the plasma to change state and thus change the ACF.

In order to start we will first develop the range ambiguity which is due to the pulse shape and receiver filter on the ISR systems. If we look at data received by the ISR system at time n, with a wavenumber $\mathbf{k}$ and pulse shape $s(n)$, noted as $x(n)$ we can see that the received signal can be represented as the following

$$x(n) \propto h(n) * \int_{\mathbf{r}} e^{-j\mathbf{k}\cdot\mathbf{r}} s(n - \frac{2r}{c}) n_e(\mathbf{r}, n) d\mathbf{r}, \tag{2}$$

where $h(n)$ is the receiver filter, $n_e(\mathbf{r}, n)$ is the electron density fluctuation. Generally it is assumed that the pass band of the filter is larger then the bandwidth of the electron density fluctuation *Kudeki* [2003]. As such it can be assumed that filter will only act on the the shape of the pulse. This will change Equation 2 to the following:

$$x(n) \propto * \int_{\mathbf{r}} e^{-j\mathbf{k}\cdot\mathbf{r}} a(n - \frac{2r}{c}) n_e(\mathbf{r}, n) d\mathbf{r} \tag{3}$$

where $a(n) = h(n) * s(n)$.

When the autocorrelation of the signal is done we find the following formula, *Nikoukar et al.* [2008].

$$\langle x(n)x^*(n+\tau)\rangle = \int_{\mathbf{r}'}\int_{\mathbf{r}} e^{-2j\mathbf{k}\cdot(\mathbf{r}'-\mathbf{r})} a(n-\frac{2r}{c}) a^*(n+\tau-\frac{2r'}{c}) \langle n_e(\mathbf{r}, n) n_e(\mathbf{r}', n+\tau)\rangle d\mathbf{r} d\mathbf{r}' \tag{4}$$

where r' is the magnitude of the vector $\mathbf{r}'$. We can make some simplifying assumption at this point that the space-time autocorrelation function of $n_e(\mathbf{r}, t)$, $\langle n_e(\mathbf{r}, n) n_e(\mathbf{r}', n+\tau)\rangle$, will vanish as the magnitude of $\mathbf{x} \equiv \mathbf{r}' - \mathbf{r}$ increases. Once the spatial correlation is removed we can rewrite Equation 4 as

$$\langle x(n)x^*(n+\tau)\rangle = \int_{\mathbf{r}} a(n-\frac{2r}{c}) a^*(n+\tau-\frac{2r}{c}) \int_{\mathbf{x}} e^{-2j\mathbf{k}\cdot\mathbf{x}} \langle n_e(\mathbf{r}, n) n_e(\mathbf{x}+\mathbf{r}, n+\tau)\rangle d\mathbf{x} d\mathbf{r}. \tag{5}$$

The inner integral is a spatial Fourier transform evaluated at the wave number of the radar $\mathbf{k}$

$$\langle |n_e(\mathbf{k}, r, \tau)|^2 \rangle \equiv \int_{\mathbf{x}} e^{-2j\mathbf{k}\cdot\mathbf{x}} \langle n_e(\mathbf{r}, b) n_e(\mathbf{x}+\mathbf{r}, n+\tau)\rangle d\mathbf{x}. \tag{6}$$

Equation 5 becomes

$$\langle x(n)x^*(n+\tau)\rangle = \int_r a(n-\frac{2r}{c}) a^*(n+\tau-\frac{2r}{c}) \langle |n_e(\mathbf{k}, \mathbf{r}, \tau)|^2\rangle dr. \tag{7}$$

It should be noted that the term $a(n)a^*(n+\tau)$ is the soft target ambiguity function. If n is replaced with $2r_s/c$ we can see that the this function represented as $W(\tau, r_s, r)$ *Nikoukar* [2010]. In order to simplify notation we will represent $\langle|n_e(\mathbf{k}, \mathbf{r}, \tau)|^2\rangle$, as $R(\mathbf{r}, \tau)$. Assuming, for the moment, that R only varies across the range dimension r we can now represent this in the form of a Fredholm integral equation

$$\langle x(2r_s/c)x^*(2r_s/c+\tau)\rangle = \int_r W(\tau, r_s, r)R(r, \tau)dr. \tag{8}$$

This function is in a way a lag dependent smoothing along the range dimension of $R(r, \tau)$.

The spatial ambiguity across angle is determined by the antenna beam pattern. In phase array radars this beam pattern is ideally the array factor multiplied by the element pattern *Balanis* [2005]. The array factor is determined by a number of things including the element spacing in both x and y (dx, dy) and the wave number of the radar, k. Making idealized assumptions with no mutual coupling and that the array elements are cross dipole elements AMISR systems will have the following array pattern for pointing angle (θ_0, ϕ_0),

$$F(\theta, \phi) = \frac{1}{2}(1+\cos(\theta)^2)\left[\frac{1}{MN}\left(1+e^{j(\psi_y/2+\psi_x)}\right)\frac{\sin((M/2)\psi_x)}{\sin(\psi_x)}\frac{\sin((N/2)\psi_x)}{\sin(\psi_x/2)}\right]^2, \tag{9}$$

where $\psi_x = -kd_x(\sin\theta\cos\phi - \sin\theta_0\cos\phi_0)$, $\psi_y = -kd_y(\sin\theta\sin\phi - \sin\theta_0\sin\phi_0)$.

This spatial ambiguity is a separable function made up of the components of $W(r,\tau)$ and $F(\theta,\phi)$. A rendering of an example of this full ambiguity function for an uncoded long pulse and antenna pattern in (9) can be seen in Figure 1

2.2. Ambiguity after Frame transformation

In order to simplify notation first assume that the autocorrelation functions have been descritized and each i^{th} lag can be represented as x_i. The measured lag product will also be represented as $y_i(\mathbf{r}_s,t_s)$. With this in mind the measurement process of the i^{th} lag by the ISR can be represented as follows,

$$y_i(\mathbf{r}_s,t_s)=\int L_i(t_s,\mathbf{r}_s,t,\mathbf{r})x_i(t,\mathbf{r})dtd\mathbf{r}. \tag{10}$$

For this we will focus on a single instance in the sampled time. We will assume that the radar is integrating over a length of time T beginning at t_0 which will be the label of the sampled time. The operator L will be represented as a separable function KI where I is an indicator function of length T and centered at $t_0+1/2$. This will change (10) to the following,

$$y_{i,t_0}(\mathbf{r}_s)=\int K_i(\mathbf{r}_s,\mathbf{r})\int_{t_0}^{t_0+T} x_i(t,\mathbf{r})dtd\mathbf{r}. \tag{11}$$

At this point it will be assumed that x_i is rigid object and does not deform with respect to $\mathbf{r}$ over time period $[t_0,t_0+T]$. Also it will be assumed that the lag will be moving with a constant velocity $\mathbf{v}$. Thus $x_i(\mathbf{r},t)\Rightarrow x_i(\mathbf{r}+\mathbf{v}t)$. At this point (11) becomes,

$$y_{i,t_0}(\mathbf{r}_s) = \int \int_{t_0}^{t_0+T} K_i(\mathbf{r}_s, \mathbf{r}) x_i(\mathbf{r} + \mathbf{v}t) dt d\mathbf{r}. \tag{12}$$

A change of variables where $\mathbf{r}' = \mathbf{r} + \mathbf{v}t$ acts as a Galilean transform and applies a warping to the kernel and changing the frame of reference. Then (12) becomes

$$y_{i,t_0}(\mathbf{r}_s) = \int \int_{t_0}^{t_0+T} K_i(\mathbf{r}_s, \mathbf{r}' - \mathbf{v}t) x_i(\mathbf{r}') dt d\mathbf{r}'. \tag{13}$$

The next step is to make the specific observation that in ISR each point of the sample spatial variable $\mathbf{r}_s$ will be the determined the m^{th} range gate and the n^{th} beam. This shows the final problem is truly a semi-discrete inverse problem and (12) becomes,

$$y_{i,t_0,m,n} = \int \left[\int_{t_0}^{t_0+T} K_{i,m,n}(\mathbf{r}' - \mathbf{v}t) dt \right] x_i(\mathbf{r}') d\mathbf{r}'. \tag{14}$$

The kernel K is actually a separable function with the component $f_{i,n}(\mathbf{r}')$ caused by the range ambiguity of the i^{th} lag at the m^{th} range gate. The function $g_m(\mathbf{r}')$ is the angle ambiguity from the n^{th} beam.

By performing the integration in t the problem can now be simplified further back to a Friedholm integral equation by simply replacing the terms in the square brackets as a new kernel A,

$$y_{i,t_0,m,n} = \int A_{i,m,n}(\mathbf{r}') x_i(\mathbf{r}') d\mathbf{r}'. \tag{15}$$

We are now left with a semi-discrete inverse problem to solve. The operator A can be estimated through knowledge of the radar system and pulse pattern which would determine the antenna beam pattern and the range ambiguity function. The velocity $\mathbf{v}$ can be estimated by taking taking measurements of the Doppler shift and using a methodology seen in *Butler et al.* [2010]. Once the operator has been determined debluring methods can be applied.

3. Simulation

In order to determine if it is possible to improve the resolution of ISR processing synthetic data was created using a known condition of a simulated ionosphere. The simulator creates data by deriving filters from the autocorrelation function and applying it to complex white Gaussian noise. In a sense every point in time and space noise plant and filter structure as in Figure 3. The data is then scaled and summed together according to its location in range and angle space to radar.

To test this a phantom ionosphere is created where a small plasma enhancement moves through the radar field of view. The background electron density varies in altitude as a Chapman function while the electron and ion temperature remains constant. This is done to avoid having to do full fit and thus only try to measure the electron density. Also estimates of the zeroth lag are only necessary. Added to this is a 35 km radius sphere of enhance electron density of about 5×10^{10} m^{-3} centered at 400 km altitude moving at 500 m/s along the y direction.

4. Possible Mitigation Techniques

5. Conclusion

References

(2005), Eiscat 3d design specification document.

(2014), Amisr overview.

Balanis, C. A. (2005), *Antenna Theory: Analysis and Design*, Wiley-Interscience.

Butler, T. W. (2013), Spatial statistics and analysis of Earth's ionosphere, Ph.D. thesis.

Butler, T. W., J. Semeter, C. J. Heinselman, and M. J. Nicolls (2010), Imaging f region drifts using monostatic phased-array incoherent scatter radar, *Radio Sci.*, *45*(5), RS5013, doi:10.1029/2010RS004364.

Dahlgren, H., J. L. Semeter, K. Hosokawa, M. J. Nicolls, T. W. Butler, M. G. Johnsen, K. Shiokawa, and C. Heinselman (2012a), Direct three-dimensional imaging of polar ionospheric structures with the resolute bay incoherent scatter radar, *Geophysical Research Letters*, *39*(5), n/a–n/a, doi:10.1029/2012GL050895.

Dahlgren, H., G. W. Perry, J. L. Semeter, J. P. St. Maurice, K. Hosokawa, M. J. Nicolls, M. Greffen, K. Shiokawa, and C. Heinselman (2012b), Space-time variability of polar cap patches: Direct evidence for internal plasma structuring, *Journal of Geophysical Research: Space Physics*, *117*(A9), A09,312, doi:10.1029/2012JA017961.

Dougherty, J. P., and D. T. Farley (1960), A theory of incoherent scattering of radio waves by a plasma, *Proceedings of the Royal Society of London. Series A, Mathematical and Physical Sciences*, *259*(1296), pp. 79–99.

Dougherty, J. P., and D. T. Farley (1963), A theory of incoherent scattering of radio waves by a plasma, 3 scattering in a partly ionized gas, *Journal of Geophysical Research*, *68*, 5473.

Farley, D. T., J. P. Dougherty, and D. W. Barron (1961), A theory of incoherent scattering of radio waves by a plasma ii. scattering in a magnetic field, *Proceedings of the Royal Society of London. Series A, Mathematical and Physical Sciences*, *263*(1313), pp. 238–258.

Gordon, W. (1958), Incoherent scattering of radio waves by free electrons with applications to space exploration by radar, *Proceedings of the IRE*, *46*(11), 1824–1829, doi:10.1109/JRPROC.1958.286852.

Hagfors, T. (1961), Density fluctuations in a plasma in a magnetic field, with applications to the ionosphere, *Journal of Geophysical Research*, *66*(6), 1699–1712, doi:10.1029/JZ066i006p01699.

Holt, J. M., D. A. Rhoda, D. Tetenbaum, and A. P. van Eyken (1992), Optimal analysis of incoherent scatter radar data, *Radio Sci.*, *27*(3), 435–447, doi:10.1029/91RS02922.

Hysell, D. L., F. S. Rodrigues, J. L. Chau, and J. D. Huba (2008), Full profile incoherent scatter analysis at jicamarca, *Annales Geophysicae*, *26*(1), 59–75, doi:10.5194/angeo-26-59-2008.

Kudeki, E. (2003), *ECE 458 Lecture Notes, Application to Radio Wave Propagation*, Univ. Of Illinois, Urbana IL.

Lehtinen, M. S. (1989), On optimization of incoherent scatter measurements, *Advances in Space Research*, *9*(5), 133 – 141, doi:http://dx.doi.org/10.1016/0273-1177(89)90351-7.

Lehtinen, M. S., and A. Huuskonen (1996), General incoherent scatter analysis and {GUISDAP}, *Journal of Atmospheric and Terrestrial Physics*, *58*(1–4), 435 – 452, doi:http://dx.doi.org/10.1016/0021-9169(95)00047-X, ¡ce:title¿Selected papers from the sixth international Eiscat Workshop¡/ce:title¿.

Lehtinen, M. S., A. Huuskonen, and J. Pirttilä (1997), First experiences of full-profile analysis with GUISDAP, *Annales Geophysicae*.

Nicolls, M. J., and C. J. Heinselman (2007), Three-dimensional measurements of traveling ionospheric disturbances with the Poker Flat Incoherent Scatter Radar, *Geophysical Research Letters*.

Nikoukar, R. (2010), Near-optimal inversion of incoherent scatter radar measurements- coding schemes, processing techniques, and experiments, Ph.D. thesis, University of Illinois at Urbana-Champaign.

Nikoukar, R., F. Kamalabadi, E. Kudeki, and M. Sulzer (2008), An efficient near-optimal approach to incoherent scatter radar parameter estimation, *Radio Science*, *43*(5), n/a–n/a, doi:10.1029/2007RS003724.

Richards, M. A. (2005), *Fundamentals of Radar Signal Processing*, McGraw-Hill.

Semeter, J., T. Butler, C. Heinselman, M. Nicolls, J. Kelly, and D. Hampton (2009), Volumetric imaging of the auroral ionosphere: Initial results from pfisr, *Journal of Atmospheric and Solar-Terrestrial Physics*, *71*, 738 – 743, doi: 10.1016/j.jastp.2008.08.014, ¡ce:title¿Advances in high latitude upper atmospheric science with the Poker Flat Incoherent Scatter Radar (PFISR)¡/ce:title¿.

Acknowledgments. (Text here)

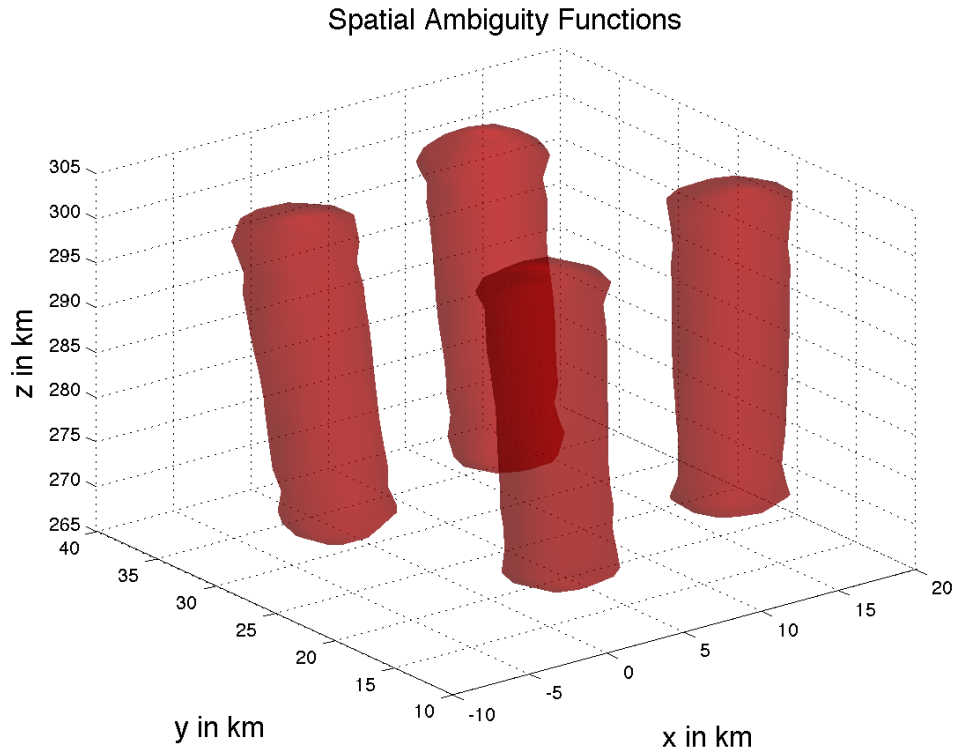

Figure 1. Full Spatial Ambiguity Function

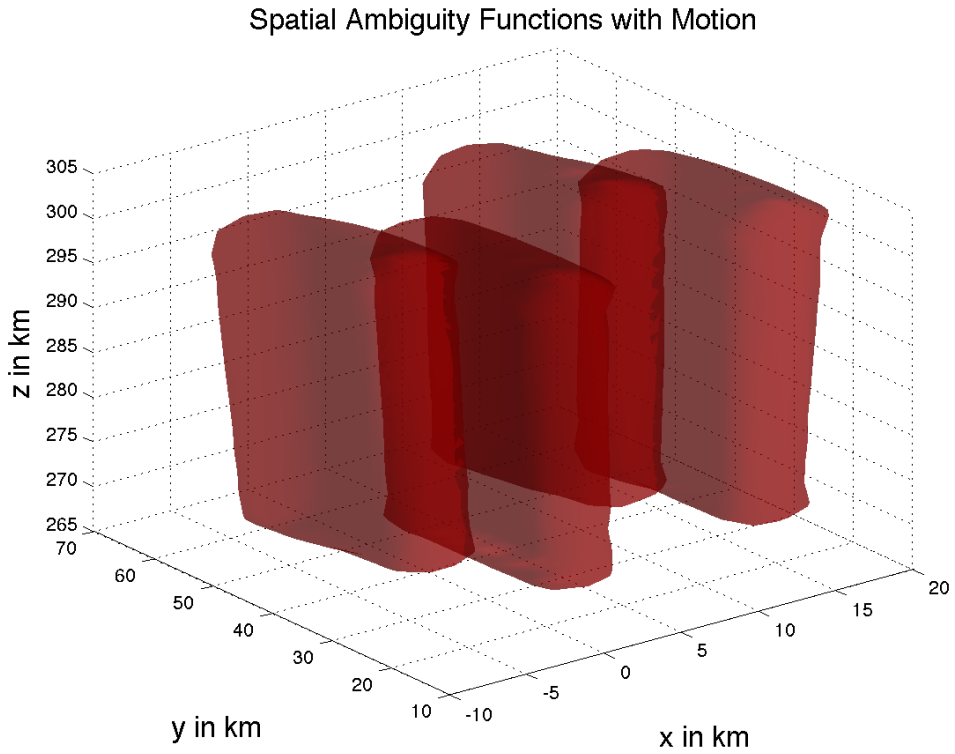

Figure 2. Full Spatial Ambiguity Function With Motion

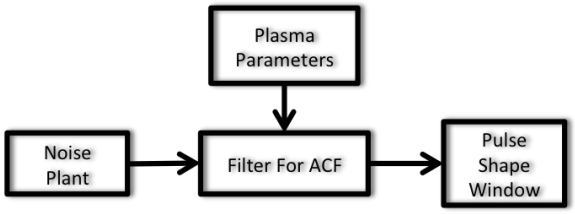

Figure 3. I/Q Simulator Diagram